

# The eutardigrade *Thulinia stephaniae* has an indeterminate development and the potential to regulate early blastomere ablations

Andreas Hejnol and Ralf Schnabel\*

Technische Universität Braunschweig, Institut für Genetik, Spielmannstrasse 7, D-38106 Braunschweig, Germany

\*Author for correspondence (e-mail: r.schnabel@tu-bs.de)

Accepted 23 December 2004

Development 132, 1349–1361  
Published by The Company of Biologists 2005  
doi:10.1242/dev.01701

## Summary

We present a detailed analysis of the cell lineage of the tardigrade *Thulinia stephaniae* with a 4D-microscopy system (3D time-lapse recording). The recording, of the entire development from embryogenesis until hatching, allowed us to analyze the fate of single descendants from early blastomeres up to germ layer formation and tissue development. The embryo undergoes an irregular indeterminate cleavage pattern without early fate restriction. During gastrulation, mesodermal and endodermal precursors, and a pair of primordial germ cells migrate through a blastopore at the prospective position of the mouth. Our results are not consistent with earlier descriptions of mesoderm formation by enterocoely in tardigrades. The mesoderm in *Thulinia stephaniae* originates from a variable number of blastomeres, which form mesodermal bands that later produce the serial somites. The nervous system is formed by neural

progenitor cells, which delaminate from the neurogenic ectoderm. Early embryogenesis of *Thulinia stephaniae* is highly regulative, even after laser ablations of blastomeres at the two- and four-cell stages ‘normal’ juveniles are formed. This has never been observed before for a protostome. Germ cell specification occurs late during development between the sixth and seventh cell generation. Comparing the development of other protostomes with that of the Tardigrada, which occupy a basal position within the Arthropoda, suggests that an indeterminate cleavage and regulatory development is not only part of the ground pattern of the Arthropoda, but probably of the entire Ecdysozoa.

Key words: Tardigrade, Ablation experiments, Indeterminate, Cell lineage, 4D-microscopy, Arthropoda, Ecdysozoa, Mesoderm

## Introduction

Most of what is known about tardigrade development and has been adopted by zoology textbooks originating from the early studies of von Erlanger (von Erlanger, 1895), von Wenck (von Wenck, 1914) and Marcus (Marcus, 1928; Marcus, 1929). However, a recent study by Eibye-Jacobsen (Eibye-Jacobsen, 1997) on tardigrade development was unable to confirm some of the conclusions of these authors. For example Marcus and von Erlanger reported that the mesoderm is formed by enterocoely from the gut, yet enterocoelic formation of mesoderm is usually found only in deuterostome animals. The interpretations of the early cleavage pattern of tardigrades are also controversial. All authors agree that tardigrades show total cleavage; however, Marcus (Marcus, 1929) interprets it as indeterminate, whereas Eibye-Jacobsen (Eibye-Jacobsen, 1997) suggests that the early cleavage pattern is consistent with a modified spiral pattern. Thus, the data matrix of the current zoology book by Brusca and Brusca (Brusca and Brusca, 2003) notes tardigrade development as being ‘fundamentally spiral’. This scarcity of information, as well as new ideas about the metazoan phylogeny, have brought the tardigrade development back into focus. According to molecular, morphological and palaeontological data (Dewel and Dewel, 1997; Garey, 2001;

Garey et al., 1996; Garey et al., 1999; Giribet et al., 1996; Giribet et al., 2000; Maas and Waloszek, 2001; Mallatt et al., 2004; Nielsen, 2001; Regier and Shultz, 2001; Schmidt-Rhaesa, 2001; Weygoldt, 1986), tardigrades are associated with the Euarthropoda, thus forming along with the onychophorans the taxon Arthropoda. But the sister group of the arthropod lineage is now questioned. The Ecdysozoa hypothesis, which is based mainly on molecular data (e.g. Aguinaldo et al., 1997; de Rosa et al., 1999; Garey, 2001; Giribet et al., 2000; Mallatt et al., 2004), favours now the Cycloneuralia or its members (Kinorhyncha, Loricifera, Priapulida, Nematomorpha and Nematoda) and not, according to the Articulata hypothesis, the Annelida as the sister group. However, the Ecdysozoa hypothesis is still debated (Giribet, 2003; Nielsen, 2003; Schmidt-Rhaesa et al., 1998; Scholtz, 2002; Scholtz, 2003) and new data are needed to resolve the problem. A comparative approach is needed to determine the ancestral mode of development in the Arthropoda, thereby preferentially serving as evidence to support one of the two hypotheses. As basal members of the arthropods, tardigrades are one of the key groups to investigate when reconstructing the ancestral mode. Therefore, we examined the early cleavage pattern and cell lineage of the eutardigrade *Thulinia stephaniae* using a 3D time-lapse microscopy system (4D microscopy)

(Schnabel et al., 1997), which allows us to follow cells in the living embryo. This new technology has been successfully used for studies of nematode embryos (Dolinski et al., 1998; Houthoofd et al., 2003; Schnabel et al., 1997), the analysis of brain development in *Drosophila* (Urbach et al., 2003), and description of segmentation in an isopod crustacean (A. Hejnl, PhD thesis, Humboldt University of Berlin, 2002) (Dohle et al., 2004). To further investigate the type of determination and the potential for regulation of the tardigrade embryo, we combined 4D-microscopy with laser cell ablations.

## Materials and methods

### Culture

*Thulinia stephaniae* is a freshwater tardigrade that can be maintained in cultures at 15°C to 25°C on an algae diet in the laboratory. Two to 12 fertilized eggs are laid into the exuvia during moulting. Cultures were obtained from Connecticut Valley Biological Supply (MA, USA). *Thulinia stephaniae* is present in the Gene Database, with partial sequences for 18S rRNA, RNA polymerase II subunit and elongation factor 1  $\alpha$ , and has been used for molecular phylogeny (Garey, 2001; Garey et al., 1999).

### 4D-microscopy

For the 4D recordings, the early eggs were removed from the exuvia with scissor needles and embryos were mounted on an agar pad under the microscope following a slightly modified protocol developed for *C. elegans* (Sulston and Horvitz, 1977). A 60×24 mm cover slip is used and the water is only around the agar pad to supply the embryo with sufficient oxygen. The fundamentals of 4D microscopy are described by Schnabel et al. (Schnabel et al., 1997). Commercial parts are now available for the microscope and high-resolution digital images can be stored. A Zeiss Axioplan Imaging 2 microscope with an internal focus drive was used to move the temperature-controlled stage to record the z-series (45 focal levels, increment 1  $\mu$ m). Pictures are captured with a Hamamatsu Newvicon camera, digitized with an Inspecta 3 frame grabber (Mikroton, Germany) and finally compressed tenfold with a wavelet function (Lurawave, Germany). Digital cameras like the PCO sensicam can also be used. The microscope is controlled with a PC using software (AK Schulz and RS) programmed in C++. Embryos were recorded at 24°C until the body plan was established (~48 hours of development). Embryos were then removed from the microscope slide and placed in culture to increase survival and hatching rates. Records were analyzed as described by Schnabel et al. (Schnabel et al., 1997), using SIMI°BioCell software (SIMI, Germany). This software manages the large quantity of digital image data generated and helps to document cell positions, migrations and mitoses during computational developmental analysis. The data are illustrated as a cell genealogy tree and the positions of the nuclei can be viewed as 3D-representations using coloured spheres (e.g. Fig. 2). Only embryos which developed normally and gave rise to hatched, normal instars were analyzed. Our analysis of normal development is based on four embryos, henceforth referred to as embryos 1-4.

### Laser ablations

Blastomeres were ablated as described by Hutter and Schnabel (Hutter and Schnabel, 1994). For cell ablations, eggs were mounted on an agar pad while still in the exuvia to allow the identification of manipulated eggs after culture. The intensity of the laser beam and the duration of treatment were optimized to ensure complete destruction of the ablated blastomere without causing lethal damage to the embryo. 4D recordings of embryos were stopped after degeneration of all descendants of the ablated cell to cytoplasts had occurred and the

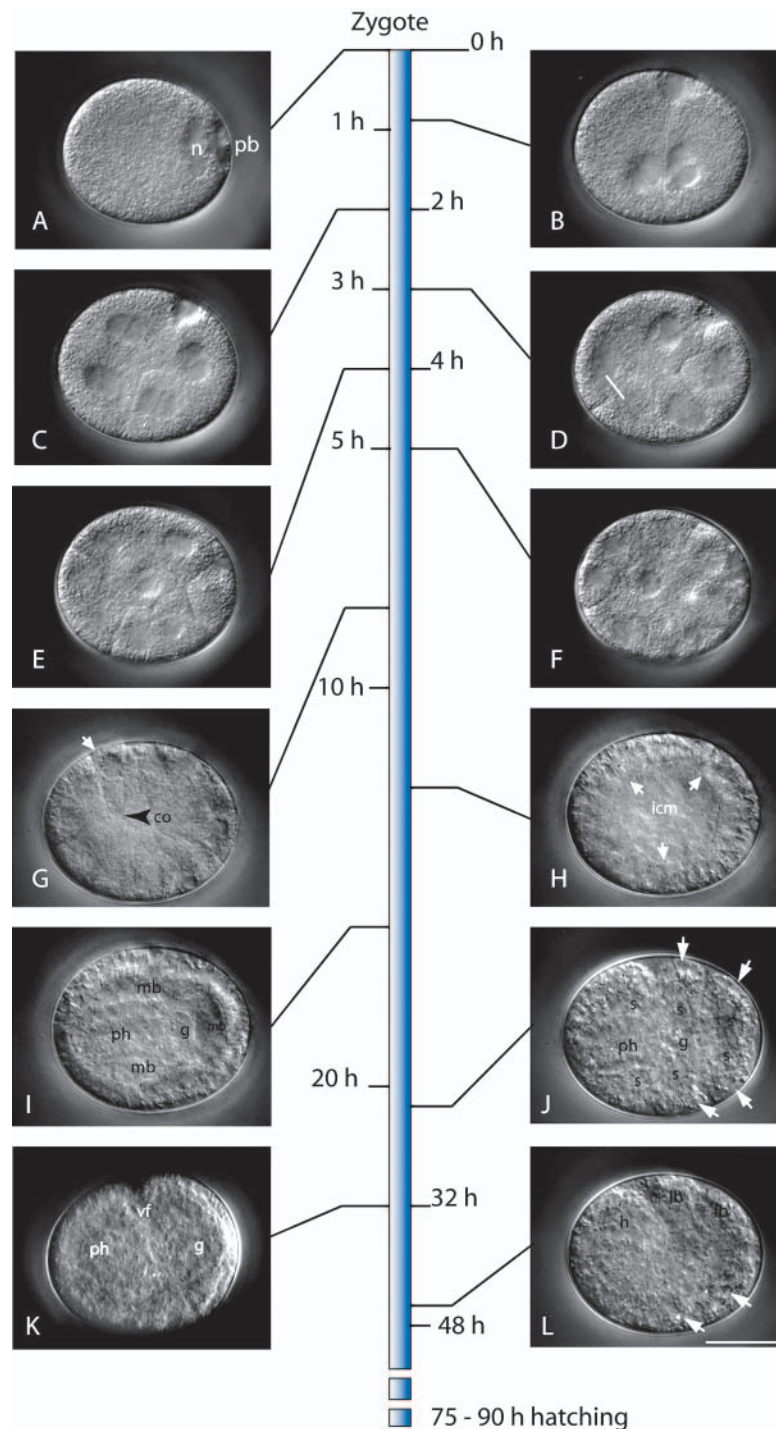
exuvia containing the embryos was incubated at 15°C until the embryos hatched.

## Results

### Early development executes an indeterminate cleavage pattern

*Thulinia stephaniae* lays fertilized eggs into its empty exuvia during moulting. The oval shaped eggs, which are about 50  $\mu$ m long and 43  $\mu$ m in diameter are completely filled by the embryo. After the eggs are deposited, the nucleus resides at the pole of the egg at which the polar body is extruded (Fig. 1A). The development is summarized in Fig. 1 (embryo 1). Blastomeres cleave totally and equally, and are indistinguishable from one another up to the onset of gastrulation. In the first cleavage the spindle is set up perpendicularly to the long axis of the egg. During the formation of the cleavage furrow, the embryo and polar body undergo a coordinated rotation of ~90° (Fig. 1B, see Movie 1 in the supplementary material). In the subsequent division to the four-cell stage, both spindles are initially oriented perpendicularly to the long axis of the egg but later rotate by 45°, allowing the blastomeres to cleave parallel to each other (Fig. 1C). After the next cell division, the relative position of the eight blastomeres varied from embryo to embryo (Fig. 1D). During the formation of the 16-cell embryo, the spindle orientation again shows variation but all mitoses occur tangential to the surface of the embryo. This cleavage pattern results in an embryo in which all blastomeres have contact with the eggshell (Fig. 1E). In some 32-cell stage embryos, we observed cell divisions that were oriented perpendicular to the surface of the embryo, which positions cells into the interior of the embryo. This could be mistaken for gastrulation. However, in all cases this 'mislocation' of the blastomere is eventually corrected through a repositioning of the cell to the surface of the embryo. In the 32-cell embryo, blastomeres polarise and the nuclei are positioned on the surface of the embryo (Fig. 1F). Blastomeres develop a pyramidal shape and the thin ends of the cells point to the inside of the embryo (Fig. 1G). After the 64-cell stage is reached, gastrulation starts with the immigration of single blastomeres. We did not observe alternating cleavage angles before the initiation of gastrulation, as is typical in spiralian cleavage (Fig. 2D-F). To determine whether specific early blastomeres have conserved positions (e.g. at the 32-cell stage and/or form conserved regions of the embryo), as it occurs in *Caenorhabditis elegans* (Schnabel et al., 1997) (see Movie 2 in the supplementary material), we differently coloured the descendants of the four-cell stage systematically with using SIMI°BioCell. In the three embryos shown in Fig. 2J-L, the distribution of cells varies from the eight-cell upwards until the 122- or 124-cell embryo and later. All attempts to match the cleavage patterns after the four-cell stage by rotating the embryos around their axes failed, thus no stereotyped pattern in the localization of the descendants of the early blastomeres was detectable. Additionally, cell migrations did not occur prior to the onset of gastrulation in the analyzed embryos. The early development of embryos 1 to 3 can be observed in Movies 3 to 5 (see supplementary material), showing 4D representations corresponding to Fig. 2J-L. The timing of the cell divisions is also variable (Fig. 2). Early embryos execute predominantly synchronous cell divisions.

**Fig. 1.** *Thulinia stephaniae* development: embryo 1. (A) In the fertilized egg the nucleus (n) is localized near the site of extrusion of the polar body (pb). (B) The first division is equal and the polar body is localized at the border of the two blastomeres. (C) Four-cell stage embryo. (D) Eight-cell stage embryo, sister blastomeres visible in this focal plane are connected with a line. (E) 16-cell embryo. (F) 32-cell stage embryo. As in earlier stages, the blastomeres are indistinguishable and all cells have contact with the surface of the embryo. (G) 64-cell stage embryo. Cells acquire a pyramidal shape, the nuclei are positioned at the surface of the embryo (white arrow). Sometimes a small blastocoel (co) is visible (black arrowhead). (H) Embryo after gastrulation. Ectodermal cells form an epithelium (white arrows) around the inner cell mass (icm) consisting of PGCs, mesoderm and endoderm precursors. (I) Germ layer differentiation and organogenesis. The gastrulated endodermal blastomeres proliferate and differentiate into the pharynx (ph) and gut (g) anlage. Mesodermal bands (mb) are located to the left and right of the endoderm. (J) Limb bud and somite formation. During differentiation of the somites (s) the ectoderm forms segmental limb buds (white arrows). The third and fourth limb buds are not in focus. The pharynx differentiates further and the gut anlage (g) consists of small cells. (K) Embryo after elongation. The ectoderm forms a ventral fold (vf) from which NPCs later delaminate to form the ganglia. The gut is surrounded by mesodermal cells, which are derived from the somites. (L) Embryo shortly before movement starts. Gut cells are vacuolized and form internal reflecting granulae (white arrows). Scale bar: 20  $\mu$ m.



However, by the fifth generation, some cells show significant retardation, which can increase to 30% of the average cell cycle by the seventh generation. Generally, the time for each cell cycle and the variability between increases as development proceeds (Fig. 2A-C).

### Gastrulation and germ layer formation in *Thulinia stephaniae*

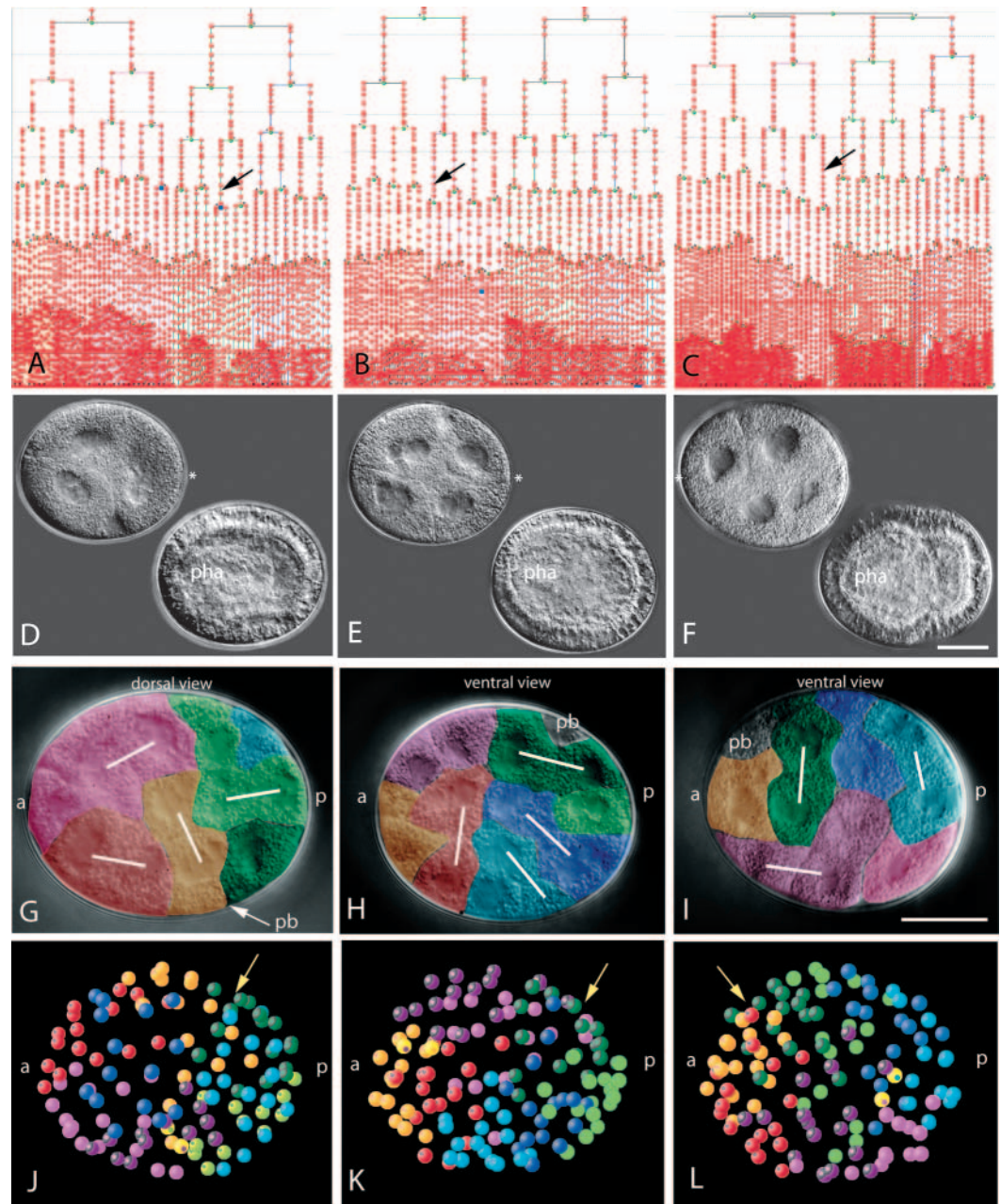
During gastrulation the main embryonic axes become visible (embryo 2, Fig. 3A). The migration of the blastomeres starts at two spatially distinct regions on the ventral surface of the embryo (Fig. 3A,B). The germ cells invaginate first through an anterior pore, the blastopore (Fig. 3F), and are immediately followed by the invagination of mesodermal and endodermal precursor cells. Interestingly, the primordial germ cells (PGC) are first encircled by the other germ layer precursors as has been described for some other arthropods (Fuchs, 1914; Kühn, 1913). Cells that migrate through the second smaller posterior pore are ectodermal cells, which after immigration rise back to the surface and fill the pore (Fig. 3D). These areas are separated by a minimum of one cell row. The origin of the germ layer precursors is variable and follows no detectable pattern in the cell lineage (Fig. 3C), indicating a non-autonomous, regional specification of these cells. After gastrulation, the mesoderm and endoderm precursors proliferate. The ectoderm is formed by cells that surround the inner cells. The cell divisions are irregular and follow no detectable pattern. The ectodermal epithelium consists of one

cell layer, which gives rise to the epidermis and the nervous system of the juvenile. After gastrulation is complete, new pores become visible at the same positions of the former pores (Fig. 3E). The anterior, larger pore forms the mouth opening (stomodaeum), and the posterior smaller pore forms the hindgut (proctodaeum) of the juvenile. Both structures are derived from ectodermal cells (Fig. 3E).

### Somite formation

We also followed the formation of the left and right anterior

**Fig. 2.** Cleavage up to the blastula stage in *Thulinia stephaniae*. The columns from left to right show embryos 1, 2 and 3 respectively. (A-C) Cell lineages from the two-cell to the 122-cell stage as viewed in SIMI<sup>o</sup>BioCell. Red dots indicate the positions where cells were marked, branches indicate mitoses. Cells divide non-synchronously and cleavage patterns differ among embryos. In the fifth generation, some cells retard their cell cycle (arrows), marking the onset of differentiation. (D-F) Four-cell and post-gastrula stages. An asterisk indicates the site of polar body extrusion (position of the spindle) upon first cleavage of the embryo. Small arrows indicate the polar body; pha marks the pharynx anlage. (G,H) Views are from the upper levels of the embryos at the 32-cell stage. Sister blastomeres are connected with lines. The descendants of the eight-cell stage embryo were coloured in Photoshop in order to visualize the cell clones. To colour code the cells in G-L, we determined the orientation of the axis at the gastrulation stage and then stained the cells and 3D-representations of nuclei (J-L) with SIMI<sup>o</sup>BioCell according to the following rules. The most anterior cell of the four-cell stage is red and its sister is pink; the most posterior cell is blue and its sister is green. At the eight-cell stage the ventral descendants were stained a darker tone than their dorsal sister cells. All 3D representations were then rotated in the same orientation (left, anterior; top, ventral surface) and ‘run’ to the 122-cell stage as shown in J,K. The division angles and blastomere arrangements differ in all embryos. Scale bar: 20  $\mu$ m in D-F.



mesodermal somites in two embryos using the 4D microscope system (embryo 1 and 3). After the mesodermal precursors enter the small blastocoel, they adhere to the inside of the outer ectodermal layer (Fig. 4A-C), on which they migrate to their final position. During this migration, the cells proliferate and form bands along the left and right side of the prospective pharynx and midgut (Fig. 4D). This proliferation does not follow a clear anteroposterior polarity and no growth zone is detectable (Fig. 4F). Later, the cells of the mesodermal bands split into groups of cells. These form segmental somites below the ectodermal prospective limb anlagen (Fig. 4E). In contrast to earlier reports (Eibye-Jacobsen, 1997; Marcus, 1928;

Marcus, 1929; von Erlanger, 1895), no cavities were detectable inside these somites during our *in vivo* observations. We were able to follow the formation of muscle from somites inside the limb bud. The remaining cells differentiated into small cells and could not be traced further.

### The nervous system is built by neuronal progenitor cells immigrating from the neurogenic ectoderm

The tardigrade central nervous system (CNS) is composed of the dorsal brain, the ventral sub-oesophageal ganglion, and the serial ventral ganglia, which are joined by connectives (Fig. 5A). In one recording (embryo 3), we could trace back

founder cells of the ventral ganglia in *Thulinia stephaniae* (Fig. 5). Before gangliogenesis is initiated (48 hours of development; Fig. 5B), the four neuronal progenitor cells (NPC), are located in the future position of the ganglia. Earlier, at 33 hours of development, the four NPCs are located in the ventral fold in an anteroposterior row ready to immigrate (Fig. 5C). The anteriormost NPC forms the first ganglion (I) the second the second ganglion (II) and so on. The four NPCs are produced between 25 and 33 hours of development, by two subsequent divisions of four precursor cells. The sisters of the NPCs founder cells in each of these two divisions differentiate into epidermis (Fig. 5D). At 25 hours, the four founders of these lineages are located in positions that are not obviously related to the final arrangement of the NPCs. For example, the founder of the most posterior NPC is in the most anterior position at this time (Fig. 5E). We could only follow the process from the left side of the embryo as embryos always rotate to the side after gastrulation. Thus, we cannot exclude the possibility that the ganglia are founded by bilaterally located NPCs, as in malacostracan crustaceans (Dohle et al., 2004). The brain of *Thulinia stephaniae* is also formed by NPCs. Although we could not determine the number of cells forming the brain, we could detect the neuroectodermal anterior region, from which the NPCs are derived (Fig. 5F). The immigration of the brain precursor occurs before the immigration of the NPCs that form the ganglia. Although the early origin of the suboesophageal ganglion remains unclear, it seems likely that it is formed by an outgrowth of the brain, as we could not detect an early anlage.

**Fig. 3.** Gastrulation of *Thulinia stephaniae*: embryo 2. (A) Ventral side of the embryo. Gastrulation initiates 9 hours after egg deposition. Posterior (arrow) of the embryo is towards the left. The PGCs migrate anteriorly through the prospective mouth opening into the embryo. (B) After 2 hours, the pores, which correspond to the prospective mouth (pm, blastopore) and anus (pan), become visible. (C) Cell lineage of the gastrulating blastomeres up to the seventh generation. The mesoderm (M, red branch) and endoderm (End, blue branch) precursors are descendants of different blastomeres. The sister cells of the PGCs (G, yellow branch) found different germ layers and the PGCs are specified in different generations. (D) Gastrulation is completed and the pores are closed (arrows). (E) The stomodaeum (stom) forms from ectodermal cells at the anterior pole (right arrow). The inconspicuous pore becomes the proctodaeum (proc, left arrow). (F) Three-dimensional reconstruction and fate map of the blastula at the 124-cell stage before onset of gastrulation. Ventral view of the anterior blastopore.

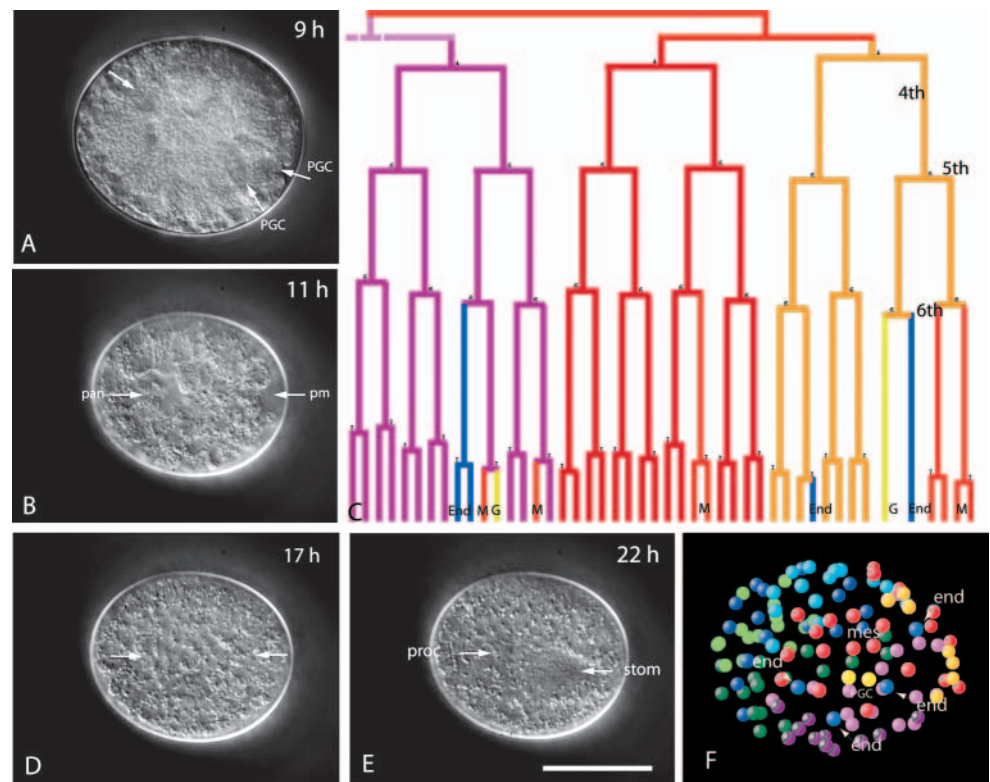
Nine mesodermal precursors (mes) are represented as red spheres. The pair of PGCs (yellow spheres) is surrounded by the germ layer precursors, including four endodermal (end) precursors (blue spheres). The remaining blastomeres acquire an ectodermal fate. Scale bar: 20  $\mu\text{m}$ .

### Specification of primordial germ cells

The germline in *Thulinia stephaniae* consists of two PGCs. In three (embryos 1, 3 and 4) out of four embryos, they could be recognized as non-dividing cells in the sixth generation before the onset of gastrulation (Fig. 6). In one embryo (embryo 2) one PGC differentiated in the sixth and the other at the seventh generation (Fig. 3C), which suggests an indeterminate specification. The PGCs are morphologically distinguishable from the somatic cells by their larger size. In all analyzed embryos, the sister cells of the PGC execute different fates (Fig. 3C, Fig. 6C). In the three embryos that form the PGCs in the sixth generation, both blastomeres of the two-cell stage form one germ cell each (Fig. 6C). In the remaining embryo, both PGCs were derived from one blastomere of the two-cell stage (Fig. 3C). These observations indicate that the PGCs are determined non-autonomously before gastrulation. During gastrulation, the germ cells migrate into the blastocoel and locate posterior to the developing pharynx, adjacent to the midgut cells (Fig. 6D). Later, during elongation of the embryo, the cells move by different paths to a posterior position, which is dorsal to the midgut, where the gonad will develop (Fig. 6E,F).

### Laser ablation of one blastomere in the two-cell stage

To test the regulatory ability of early embryos, we laser ablated blastomeres (Table 1). After ablations of one of the two blastomeres in two-cell stage embryos, normal juveniles hatched ( $n=9$ ). These juveniles, which developed from only one blastomere were smaller than the untreated control



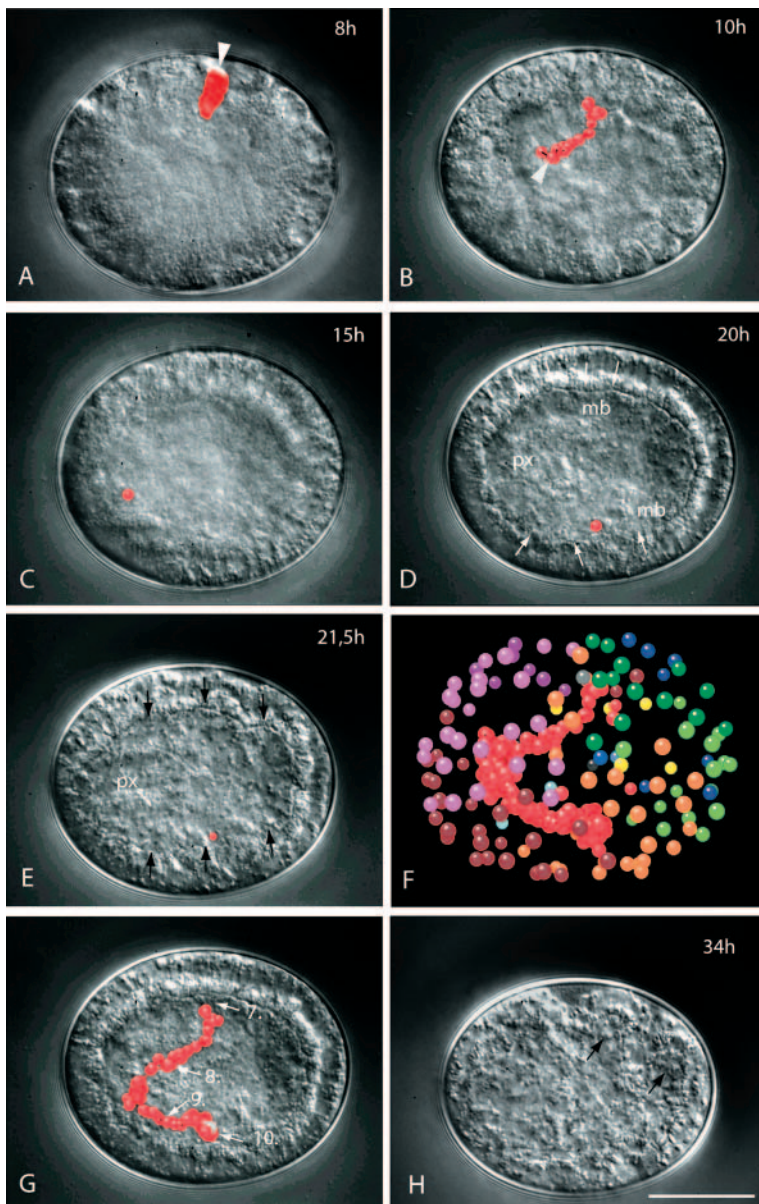


**Fig. 4.** Mesoderm development in *Thulinia stephaniae*. The genealogy of a blastomere, which contributes to the first left limb bud somite, was traced back to the precursor blastomere (embryo 1). Dorsal view, anterior towards the left. (A) Position of the mesodermal precursor shortly before it immigrates during gastrulation (arrowhead). (B) Position of traced cell 2 hours later (arrowhead). The red spheres indicate the path of migration of the cell since immigration started (projected with the migration function of the SIMI<sup>o</sup>BioCell software). (C) After the next division, the cell (red sphere) touches the anterior inner side of the ectodermal epithelium. (D) Twenty hours after egg deposition, the mesodermal bands (mb) form out of the mesodermal precursors. The mesodermal bands (arrows) stretch from posterior to anterior along the pharynx (px) and gut anlagen. The red sphere marks the position of the traced cell. (E) Embryo 1.5 hours later. The mesodermal bands form somites left and right from the gut; no cavities can be seen (black arrows). The traced cell has divided once and participates in the formation of the left second somite. (F) Three-dimensional representation of the nuclei in the 122-cell stage embryo. The row of red spheres shows the path of migration of the traced mesoderm cell. (G) Positions of the mesoderm precursor during gastrulation. The white arrows indicate the position of the precursor during specified mitoses. Later, the cell migrates along the inner epithelium of the ectoderm. (H) Embryo 34 hours after egg deposition. Mesodermal cells proliferate into the limb buds (arrows). Scale bar: 20  $\mu\text{m}$ .

#### Ablations in the four-cell stage embryo

We ablated individual blastomeres located either laterally or at one pole of the egg in four-cell embryos. Development of these embryos proceeded as described for the ablations experiments in the two-cell embryos. Normal juveniles developed from the ablated four-cell embryos, also formed a pair of two germ cells and hatched (Fig. 8, see Fig. 10). Additionally, we ablated two blastomeres, which are non-sibling in the four-cell embryo (Table 1, Fig. 9). These two embryos developed similarly to the other ablated embryos, although the development of the embryos took longer. For example, the formation of the pyramidal cells, which are normally formed prior to gastrulation, was delayed.

However, the early cell cycles proceeded normally in this developmental phase (Fig. 9A). Presumably, the delay is caused by the large aggregation of ablated cells, which occupies the centre of the embryo after ablation and which must be subsequently displaced by the untreated blastomeres in order to form the embryo (Fig. 9B,C). After the blastomeres have assembled, gastrulation starts immediately. These observations indicate an astonishing plasticity of early embryogenesis. Both embryos were recovered after the initial recording and developed into normal hatched juveniles despite the early ablations.

## Discussion

### General course of embryogenesis

For a long time, the nature of tardigrade development has remained obscure. Early descriptions have not been reinvestigated, owing to a loss of interest in 'minor phyla' and

embryos (see Fig. 10C,D). In all recorded embryos the ablated cell divided twice before the damaged descendants degraded into many cytoplasts of different size (Fig. 7A). The development of the non-ablated blastomeres was not affected (Fig. 7C). The normal cells initially surround the ablated cytoplasts (Fig. 7B), but soon begin to 'ignore' the debris and assume the typical pyramidal shape (Fig. 7A). After the blastomeres have rearranged, gastrulation is initiated (Fig. 7D). These embryos still form all tissues; the inner blastomeres form gut, mesodermal bands and the pharynx (Fig. 7E,F; Fig. 10). The ectodermal cells are much larger than in the control embryos, as it is expected for an embryo composed of only half the number of cells of a normal embryo. We did not find a compensatory cell generation in the ablated embryos during the 4D analyses. Interestingly, all ablated embryos display two germ cells. Thus, germline formation is regulative, which makes it unlikely that a pre-existing germ cytoplasm is shunted into specific blastomeres (Fig. 7E).

the experimental opportunities available in other, more tractable, systems. Therefore, the work of a sole investigator Marcus (Marcus, 1929) has appeared in nearly every invertebrate textbook for the past 70 years. We have now analyzed *Thulinia stephaniae* as a representative species for eutardigrade development using 4D microscopy. The early cleavages of the embryo are variable from the second cell division onwards. The position of the anterior posterior axis varies in relation to early cleavages. With the ability to trace the fate of single blastomeres, we could establish lineages of different embryos and show a variable origin of the PGCs and of the main germ layers. This is consistent with the impressive regulative potential of the embryo. The formation of the nervous system, especially the synchronous immigration of neural progenitor cells, resembles development patterns in some arthropods (Dove and Stollewerk, 2003; Stollewerk, 2002). Additionally, our reassessment of gastrulation and mesoderm formation displays striking similarities to these processes in some other arthropods (Anderson, 1973; Siewing, 1969). Gastrulation takes place at the ventral surface of the embryo and the blastopore corresponds to the future mouth opening. Concerning AP axis formation, gastrulation, endoderm formation and germline development, our findings are inconsistent with the descriptions of Marcus (Marcus, 1928; Marcus, 1929) and von Erlanger (von Erlanger, 1895). Eibye-Jacobsen (Eibye-Jacobsen, 1997) was not able to confirm that the mesoderm is derived from outpocketings of the gut (enterocoely), as described by Marcus (Marcus, 1928; Marcus, 1929), but she was not able to determine the origin of the mesoderm. Our lineage analysis now shows that the mesodermal somites are derived from subdivisions of lateral mesodermal bands. As opposed to Marcus (Marcus, 1928; Marcus, 1929), we find that in *Thulinia stephaniae*, all germ layers precursors are present during gastrulation. Disparities between our findings and Marcus' results may be explained by his inability to analyze the cell borders in as great of detail as his drawings suggest. Marcus himself conceded that he could not detect cell borders in the stages that follow gastrulation, yet he included cell borders in his schematic drawings (Marcus, 1928). The arrangement of the germ layer precursors that encircle the PGCs prior to immigration shows striking similarities to that of total cleaving crustacean embryos like that of the copepod *Megacyclops viridis* (Fuchs, 1914) and the water flea *Polyphemus* (Kühn, 1913). This may reflect a common fate determination mechanism in arthropods, although these crustaceans show a stereotyped cleavage program. Recent detailed cell lineage studies of amphipod embryos (Gerberding et al., 2002; Wolff and Scholtz, 2002) show a similar pattern in the arrangement of the germ cell and mesoderm and endoderm precursors. However, the cleavage

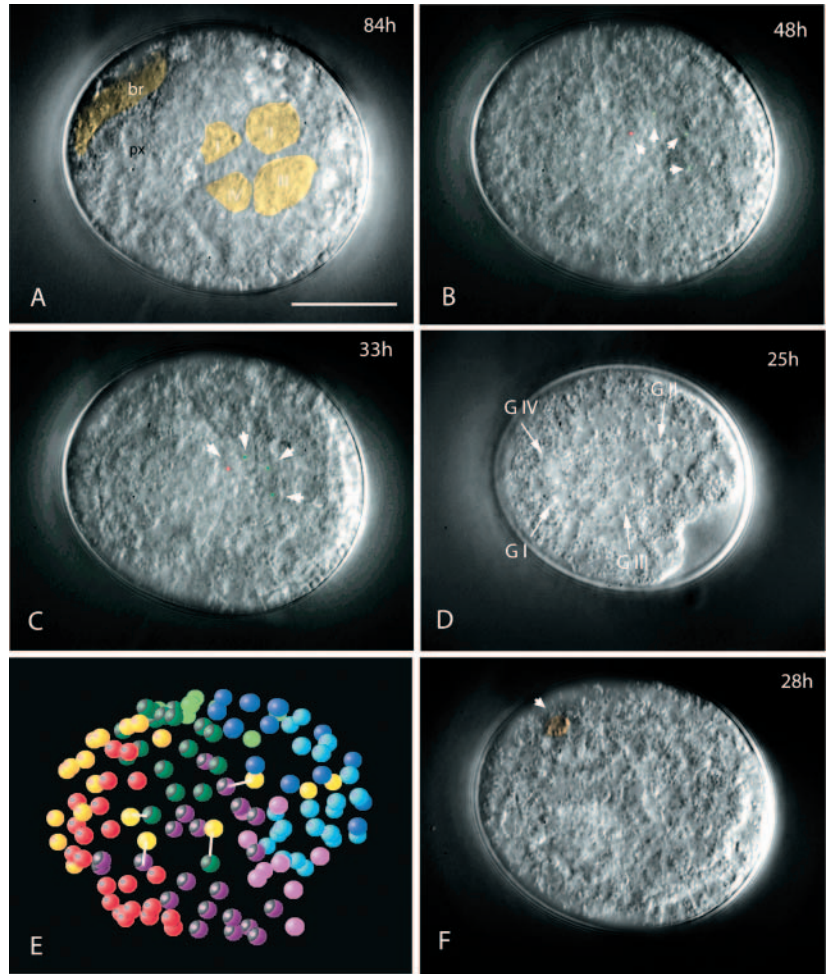


**Fig. 5.** Neurogenesis of *Thulinia stephaniae*: embryo 3. (A) Lateral view of an embryo that begins muscle contractions. The brain (br) and the ventral ganglia (I-IV) are highlighted in yellow. (B) Earlier lateral view of the same embryo after delamination of the neuronal precursor cells (arrows) and during formation of the ganglia. (C) Lateral view 15 hours earlier. After two cell divisions, the NPC are formed from the precursors. They are located in the ectodermal ventral fold inferior the future position of the ganglia. (D) Earlier ventral view. The arrows indicate the location of the NPCs in the 248-cell embryo. (E) Three-dimensional representation of the positions of the nuclei at this stage. The bright yellow spheres correspond to the NPCs, which are connected with white bars to their sister cells. Colour code see Fig. 2. The NPCs are descendants of both blastomeres of the two-cell stage. (F) View of the left side of the embryo after it has rotated at 28 hours. We followed one brain precursor (arrow) delaminating from the anterior dorsal ectoderm to start brain formation, prior to the delaminating NPCs, which form the ganglia. Scale bar: 20  $\mu$ m.

program of the amphipods is highly derived in the crustaceans and thus makes it difficult to compare. In many arthropods, lateral mesodermal bands are formed by a posterior growth zone, which proliferates towards the anterior pole (Anderson, 1973). Later coelomic cavities, also called somites, are built up by schizocoely (Anderson, 1973; Dohle, 1979). *Thulinia stephaniae* shows similarities to the pattern of mesoderm formation of the Euarthropoda and onychophorans (Manton, 1949) and therefore may reflect the ancestral condition of this process in arthropods.

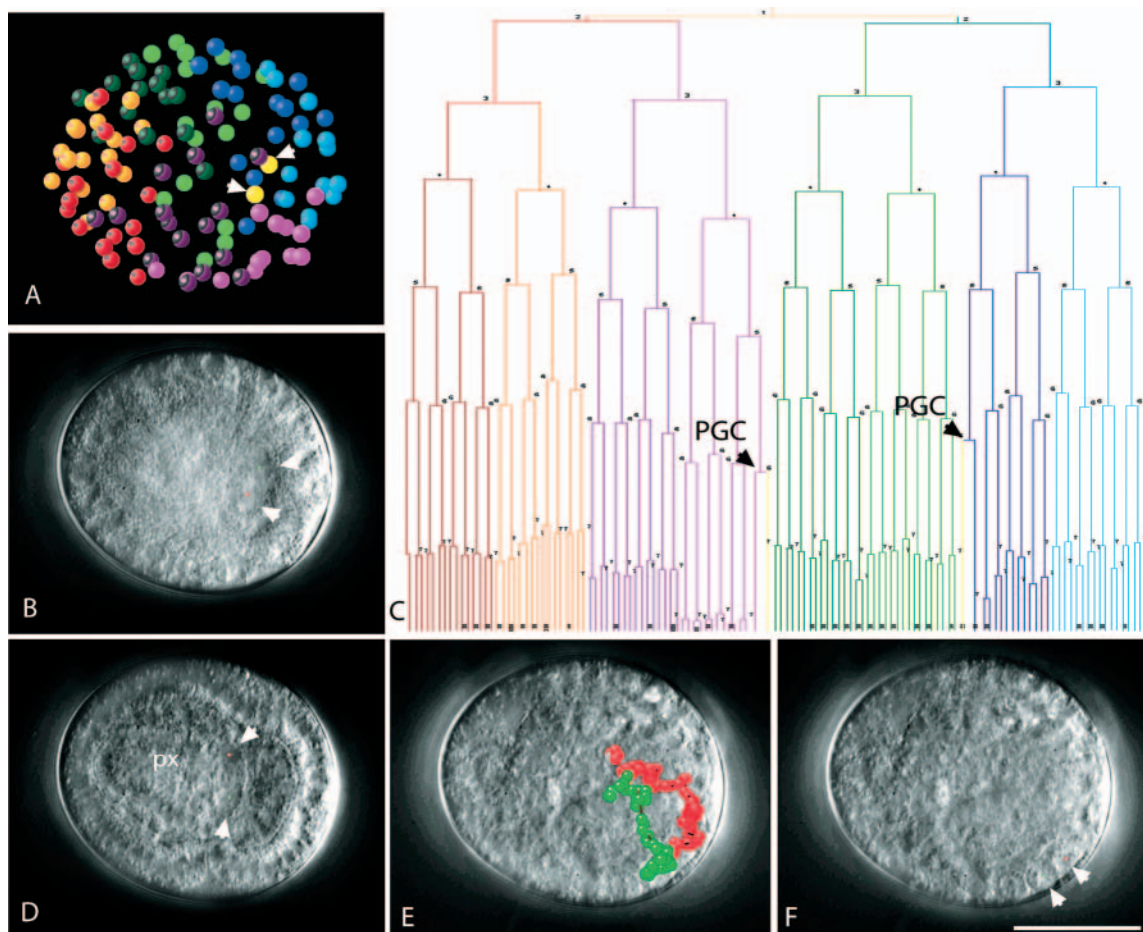


**Fig. 6.** Development of the germ cells in *Thulinia stephaniae*: embryo 3 (A) Three-dimensional representations of the positions of the primordial germ cells (PGC) (yellow spheres, arrows) after differentiation has occurred (last cell division). The neighbouring cells have large nuclei and are located at the site of the future blastopore. (B) The PGCs gastrulate (arrows). (C) The cell lineage analysis shows that the PGCs differentiated after the sixth cell division and are derived from both blastomeres of the two-cell stage. (D) Ventral view of the embryo, anterior towards the left. The PGCs are located posterior to the pharynx (px) and ventral to the midgut anlage. (E) Projection of the migration paths of the PGCs using SIMI°BioCell. During elongation of the embryo, the PGCs begin to migrate along independent paths to the prospective position of the gonad (left PGC green, right PGC red). (F) Final position of the PGCs (arrow) at the location where the gonad develops. Scale bar: 20  $\mu\text{m}$ .

**Table 1. Blastomere ablation experiments**

	Two-cell stage	Four-cell stage (one cell)		Four-cell stage (two cells)	Control
Ablation					
Exuvia 1	3	–	–	–	2
Exuvia 2	1	1	1	–	2
Exuvia 3	–	1	1	–	1
Exuvia 4	3	–	–	–	1
Exuvia 5	1	1	1	–	2
Exuvia 6	2	–	–	–	1
Exuvia 7	2	1	–	–	2
Exuvia 8	–	–	–	2	1
Single records	2	2	2	–	–
Total	14 (9)	11 (10)		2 (2)	12 (12)

Numbers in brackets indicate the number of juveniles that hatched after the ablations. Exuvia in which the untreated control embryos did not hatch were discarded.



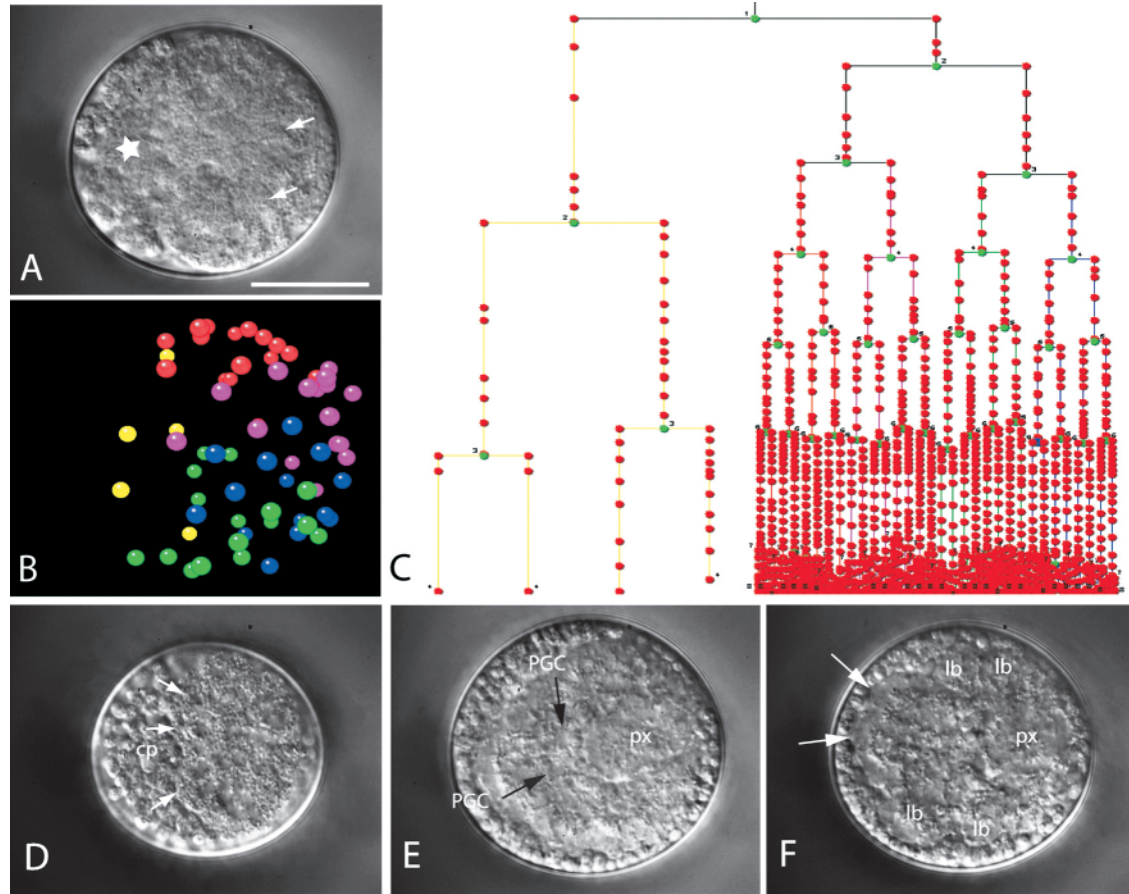


**Fig. 7.** Development after laser ablation of one blastomere in the two-cell embryo. (A) 64-cell embryo. The ablated cell cleaved twice before its descendants degraded into small cytoplasts (star). The untreated blastomeres divided normally and the descendants acquire a pyramidal shape at the 124-cell stage (arrows). (B) Three-dimensional representation of the embryo shown in A. The non-ablated descendants first surround the remaining cytoplasts (yellow spheres) of the ablated cell, but are later found further from them. (C) Lineage of the embryo up to the 64-cell stage. The non-treated blastomeres undergo normal cell cycles. (D) Later stage of the embryo. The descendants of the non-treated blastomere form an epithelium (arrows) at the border of the cytoplasts (cp). (E) Later stage of the recorded embryo. A pair of PGCs is present and the embryo develops the main organs e.g. pharynx (px). The small embryo is surrounded by the cytoplasts. (F) Stage of limb bud (lb) formation. Anterior is towards the right. The cells of the ectoderm (arrows) are much larger than those found in normal embryos at the same stage. Scale bar: 20  $\mu\text{m}$ .

### Cell ablation experiments show a high regulatory potential of the tardigrade embryo

Our cell ablation experiments indicate that early cell fate restrictions do not occur in tardigrade development. Our observations in *Thulinia stephaniae* are inconsistent with a spiral development. After our cell ablations in the two- and four-cell embryos, all embryonic axes were formed. Thus, the axes are not fixed at these stages. Despite the fact that up to one half of the embryo is missing after the ablations, germ layer formation and germ-line specification proceeded normally. No protostome embryo with a similar regulative ability to compensate for such invasive blastomere deletions has yet been reported. The highest capability for regulation in protostomes was described by Wiegner and Schierenberg (Wiegner and Schierenberg, 1999) for the nematode *Acrobeloides nanus*. Here, the posterior but not the anterior blastomere of the two-cell stage will form a larvae when the other cell is ablated. Our results suggest that a non-autonomous mechanism specifies the main axes and tissues of the embryo

sometime after the tardigrade embryo has reached the four-cell stage. It would be interesting to determine molecular mechanisms governing embryogenesis in tardigrades. However, owing to the specific biology of the system, it appears that it would be difficult to establish *Thulinia stephaniae* as a molecular genetic system allowing functional analysis.

### Phylogenetic considerations

The early development of arthropods is diverse, ranging from total cleavage to syncytial cleavage (Anderson, 1973; Scholtz, 1997; Siewing, 1969) and it has remained unclear which type of development reflects the ancestral mode. We showed for *Thulinia stephaniae*, as a representative of the tardigrades, a variable cleavage pattern with a high regulatory potential of the early embryo. Tardigrades are a basal lineage in the arthropods (Dewel and Dewel, 1997; Garey, 2001; Garey et al., 1996; Garey et al., 1999; Giribet et al., 1996; Maas and Waloszek, 2001; Mallatt et al., 2004; Nielsen, 2001; Regier and Shultz,

2001), but this does not necessarily mean that our descriptions reflect the ancestral condition in the Arthropoda. A comparison of the different types of development present in arthropods with that of the sister group of the Arthropoda (outgroup comparison), is needed to define the ground pattern (Ax, 1984; Scholtz, 2004). The classical Articulata hypothesis favours the Annelida, which display an exemplary spiral quartet cleavage, as the sister group of the Arthropoda. The cleavage program of the molluscs, the sister group of the Articulata, is also spiral. Thus, the common ancestor of the Articulata must have had a spiral cleavage, which was then modified in the stem species of the Arthropoda (Scholtz, 1997; Fig. 10A). Although several total cleaving arthropods, mainly crustaceans with a determinate cleavage and traceable cell lineage, have been investigated (Alwes and Scholtz, 2004; Anderson, 1969; Gerberding et al., 2002; Hertzler, 2002; Hertzler and Clark, 1992; Hertzler et al., 1994; Wolff and Scholtz, 2002; Zilch, 1978; Zilch, 1979), none of them shows clear traits of a spiral cleavage. The emerging Ecdysozoa hypothesis favours not the

Annelida but the Cycloneuralia (Cycloneuralia consist of Nematoda, Nematomorpha, Priapulida, Kinorhyncha and Loricifera) as the sister group of the arthropods (Aguinaldo et al., 1997; de Rosa et al., 1999; Giribet et al., 2000; Schmidt-Rhaesa et al., 1998; Valentine, 1997). This makes it unnecessary to assume that a modified spiral cleavage is part of the ground pattern of the arthropods, as no spiral cleaving cycloneuralian embryo is known. Priapulids show a 'radial' cleavage type (Lang, 1953; Zhinkin, 1949; Zhinkin and Korsakova, 1953), and the cleavage of the Nematomorpha was reported to be indeterminate (Inoue, 1958; Malakhov and Spiridonov, 1984; Meyer, 1913; Mühldorf, 1914). The sister group of the Nematomorpha, the nematodes, show diverse cleavage types. The stereotypic cleavage pattern found in *Caenorhabditis elegans* (Sulston et al., 1983), is not typical for nematodes, as several indeterminately cleaving nematode embryos have also been reported (Voronov, 1999; Voronov, 2001; Voronov and Panchin, 1998). Considering the Nematomorpha as the outgroup, a variable cleavage pattern

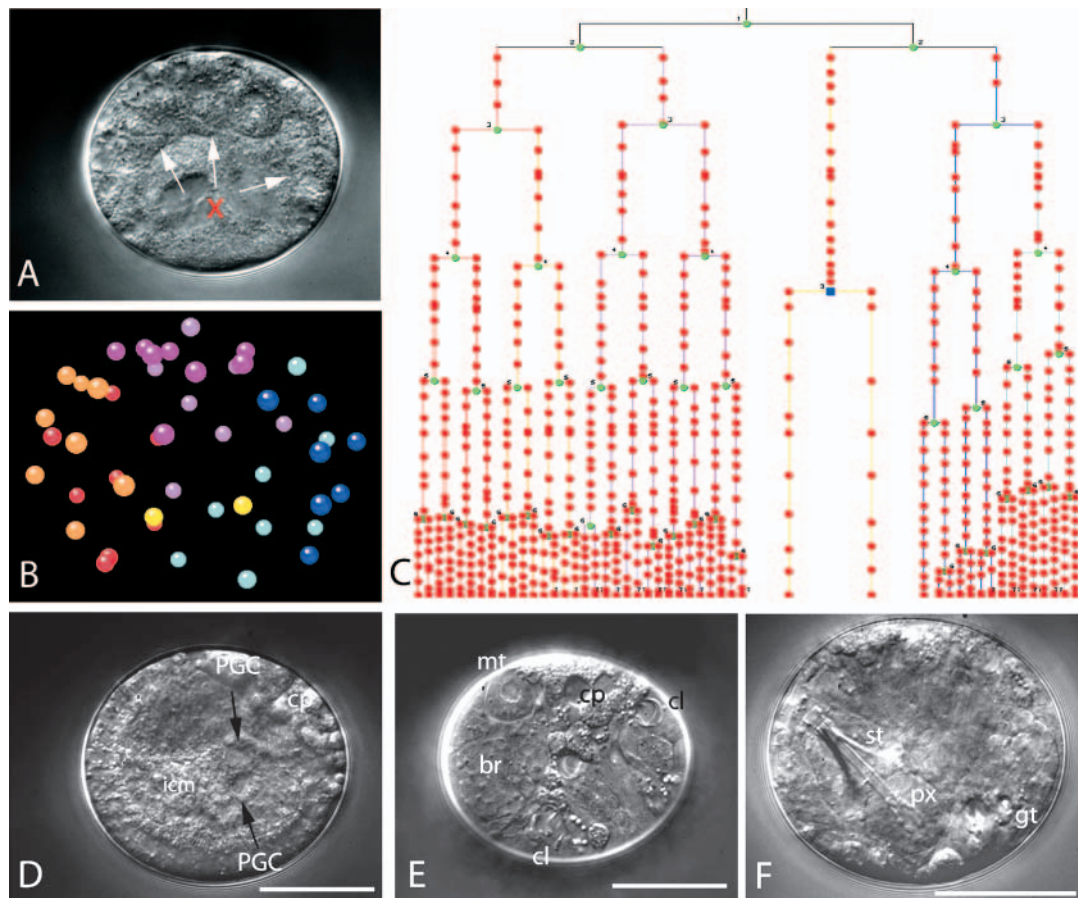


**Fig. 8.** Development after laser ablation of one cell in the four-cell stage embryo. (A) Forty-seven descendants of the untreated blastomeres surround (arrows) the ablated cell (x), which has divided once. The descendants degrade later into small cytoplasts. (B) Three-dimensional representation of the embryo shown in A, the yellow spheres mark the position of the two descendants of the ablated cell. The colour code is the same used in C. (C) Lineage of the 47-cell stage. As in a normal embryo of the corresponding stage (64-cell stage), some cell cycles are retarded. (D) Later stage after degradation of the ablated cell. The descendants of the living cells form a typical epithelium, and surround an inner endodermal cell mass (icm). The cytoplasts (cp) of the ablated cell are excluded. Two PGCs are found at the normal position (arrows). (E) Embryo before hatching. Mouth (mt), brain (br) and claws are present and look normal. The cytoplasts (cp) of the ablated cell surround the embryo. (F) Same stage as E under a higher magnification. The stylet (st), buccal tube and pharynx (px) are formed normally. The gut cells (gt) contain the typical granulae. Scale bar: 20  $\mu\text{m}$ .

**Fig. 9.** Development after ablation of two cousin blastomeres during the four-cell stage. (A) Lineage of the remaining two untreated blastomeres. The central lineage reflects the behaviour of the ablated blastomeres. The untreated blastomeres divide normally and show retarded cell cycles during the fifth generation (arrow). (B) Embryo at the 59-cell stage. (C) Three-dimensional representation of the nuclei positions of B. The descendants of the untreated blastomeres surround the ablated blastomeres. (D) Exuvia with the three embryos. In the embryos to the left and right, the ablated cells are marked with a cross. Sister cells are connected with a line. The embryo in the centre is a control embryo. (E) Later stage of D. Both treated embryos have a developed pharynx (white arrowheads). The control egg has already developed further. (F) Higher magnification of the left most embryo. Both PGCs are visible at the expected location for a normal embryo (black arrows). Scale bar: 20  $\mu\text{m}$ .

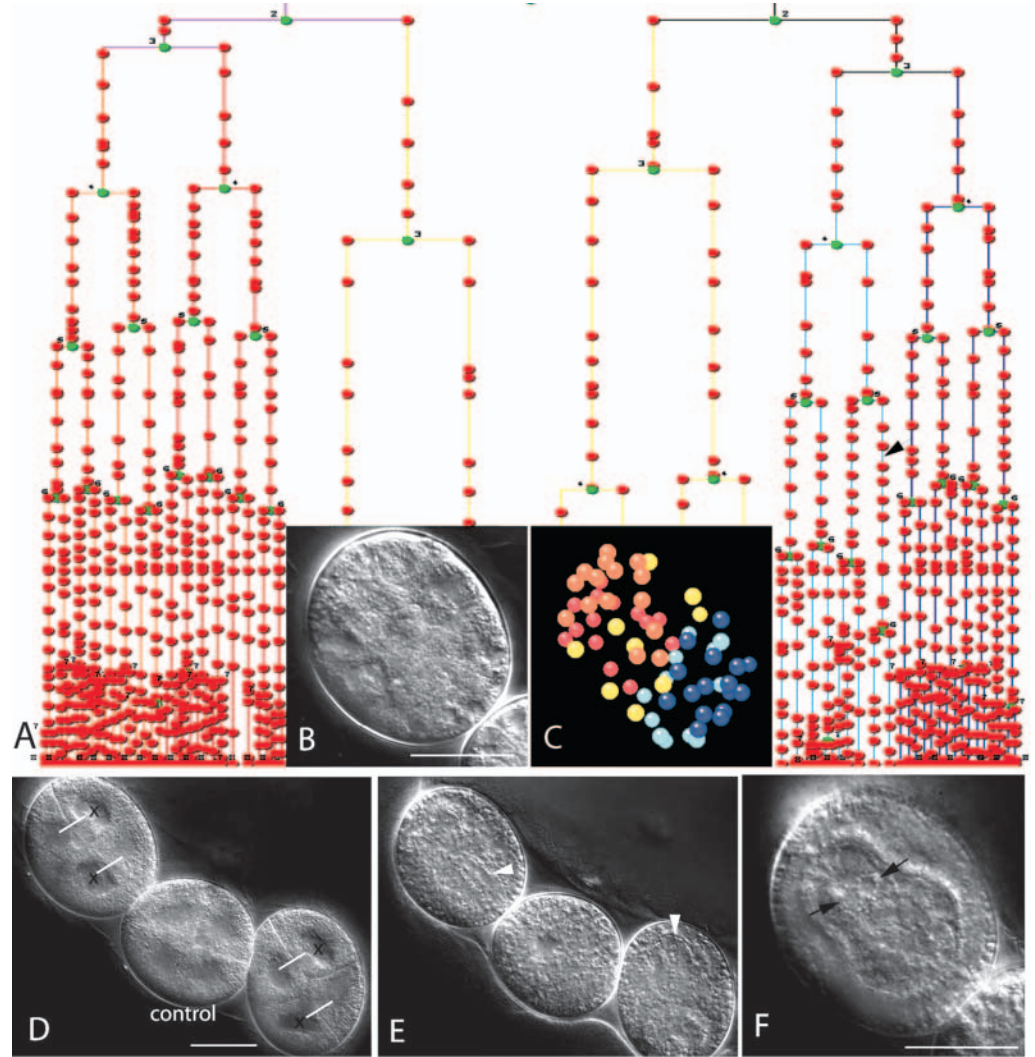
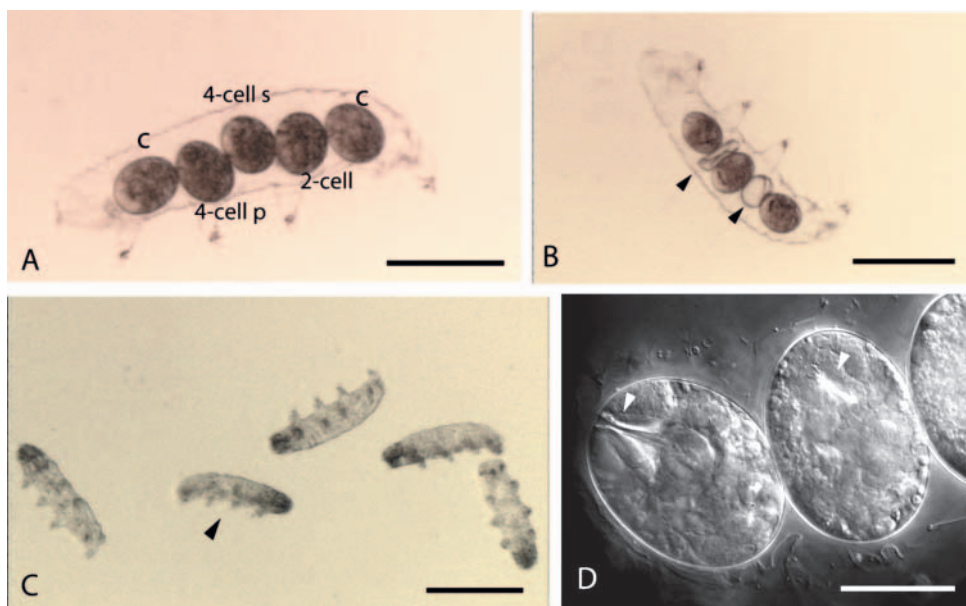


**Fig. 10.** Juveniles formed after cell ablations in the embryo. (A-C) The same exuvia. (A) Three embryos were ablated. Two control embryos are marked with 'c'. In the embryo (4-cell p) a polar blastomere and in the embryo labelled (4-cell s) a lateral blastomere have been ablated in the four-cell stage. In the third embryo (2-cell), one blastomere was ablated in the two-cell embryo. (B) Two empty eggshells (arrowheads) indicate that two juveniles have already hatched. (C) All juveniles have hatched from the exuvia and are in an anoxybiotic state. The smallest juvenile is derived from the cell ablation at the two-cell stage (arrow). (D) Embryos from a different ablation experiment at higher magnification. Left, a control embryo; right, an embryo after one cell was ablated in the two-cell stage. The stylet (white arrowhead) of the ablated embryo is reduced in comparison with that of the control embryo. Scale bars: A,B,C, 50  $\mu\text{m}$ ; D, 25  $\mu\text{m}$ .



appears to be the ancestral condition in the Nematoda, and the 'typical' stereotyped cell lineage of the rhabdite nematodes is derived (Fig. 10B). Nothing is known about the cleavage of the remaining cycloneuralian clades, the kinorhynchs and loriciferans. If the Cycloneuralia are the sister group to the Arthropods, an indeterminate cleavage pattern, similar to that of *Thulinia stephaniae*, should be part of the ground pattern in the Ecdysozoa (Fig. 10B). This notion is also supported by the fact that arthropods with an irregular cleavage pattern have been described in both crustaceans (Benesch, 1969; Scheidegger, 1976; Weygoldt, 1960) and myriapods (Dohle, 1964; Tiegs, 1940; Tiegs, 1947). Of all investigated arthropods, these species show the greatest similarity to the early development of *Thulinia stephaniae* and are thus good candidates to represent the ancestral mode of early developmental patterns in the Euarthropoda.

We thank Reinhard Møbjerg Kristensen for species identification and his help in collecting *Echiniscoides sigismundii*, which unfortunately did not want to be recorded. A field-collecting trip for *Echiniscoides sigismundii* was supported by the COBICE program of the European Union. We thank Heather Marlow, Gemma Richards, Ryan Viveiros, Gerhard Scholtz and Wolfgang Dohle for improving the manuscript.

### Supplementary material

Supplementary material for this article is available at <http://dev.biologists.org/cgi/content/full/132/6/1349/DC1>

### References

- Aguinaldo, A. M., Turbeville, J. M., Linford, L. S., Rivera, M. C., Garey, J. R., Raff, R. A. and Lake, J. A. (1997). Evidence for a clade of nematodes, arthropods and other moulting animals. *Nature* **387**, 489-493.
- Alwes, F. and Scholtz, G. (2004). Cleavage and gastrulation of the euphausiacean *Meganocyphanes norvegica* (Crustacea, Malacostraca). *Zoomorphology*, **123**, 125-137.
- Anderson, D. T. (1969). On the embryology of the cirripede crustaceans *Tetraclita rosea* (Krauss), *Tetraclita purpurascens* (Wood), *Chthamalus antennatus* (Darwin) and *Chamaesipho columna* (Spengler) and some considerations of crustacean phylogenetic relationships. *Philos. Trans. R. Soc. B* **256**, 183-235.
- Anderson, D. T. (1973). *Embryology and Phylogeny in Annelids and Arthropods*. Oxford, UK: Pergamon Press.
- Ax, P. (1984). *Das phylogenetische System*. Stuttgart, Germany: Gustav Fischer.
- Benesch, R. (1969). Zur Ontogenie und Morphologie von *Artemia salina* L. *Zool. Jb. Anat.* **86**, 307-458.
- Brusca, R. C. and Brusca, G. J. (2003). In *Invertebrates*, p. 892. Sunderland, MA: Sinauer Associates.
- de Rosa, R., Grenier, J. K., Andreeva, T., Cook, C. E., Adoutte, A., Akam, M., Carroll, S. B. and Balavoine, G. (1999). Hox genes in brachiopods and priapulids and protostome evolution. *Nature* **399**, 772-776.
- Dewel, R. A. and Dewel, W. C. (1997). The place of tardigrades in arthropod evolution. In *Arthropod Relationships* (ed. R. A. Fortey and R. H. Thomas), pp. 109-123. London, UK: Chapman & Hall.
- Dohle, W. (1964). Die Embryonalentwicklung von *Glomeris marginata* (Villers) im Vergleich zur Entwicklung anderer Diplopoden. *Zool. Jb. Anat.* **81**, 241-310.
- Dohle, W. (1979). Vergleichende Entwicklungsgeschichte des Mesoderms bei Articulaten. *Fortschr. Zool. Syst. Evolutionsforsch.* **1**, 120-140.
- Dohle, W., Gerberding, M., Hejnol, A. and Scholtz, G. (2004). Cell lineage, segment differentiation and gene expression in Crustaceans. In *Evolutionary Developmental Biology of Crustacea* (ed. G. Scholtz), pp. 95-133. Lisse, The Netherlands: A. A. Balkema.
- Dolinski, C., Borgonie, G., Schnabel, R. and Baldwin, J. G. (1998). Buccal capsule development as a consideration for phylogenetic analysis of Rhabditida (Nemata). *Dev. Genes Evol.* **208**, 495-503.
- Dove, H. and Stollewerk, A. (2003). Comparative analysis of neurogenesis in the myriapod *Glomeris marginata* (Diplopoda) suggests more similarities to chelicerates than to insects. *Development* **130**, 2161-2171.
- Eibye-Jacobsen, J. (1997). New observations on the embryology of the Tardigrada. *Zool. Anz.* **235**, 201-216.
- Fuchs, F. (1914). Die Keimblätterentwicklung von *Cyclops viridis* Jurine. *Zool. Jb. Anat.* **38**, 103-156.
- Garey, J. R. (2001). Ecdysozoa: the relationship between Cycloneuralia and Panarthropoda. *Zool. Anz.* **240**, 321-330.
- Garey, J. R., Krotec, M., Nelson, D. R. and Brooks, J. (1996). Molecular analysis supports a tardigrade-arthropod association. *Invert. Biol.* **115**, 115-121.
- Garey, J. R., Nelson, D. R., Mackey, L. Y. and Li, J. (1999). Tardigrade phylogeny: congruency of morphological and molecular evidence. *Zool. Anz.* **238**, 205-210.
- Gerberding, M., Browne, W. E. and Patel, N. H. (2002). Cell lineage analysis of the amphipod crustacean *Parhyale hawaiiensis* reveals an early restriction of cell fates. *Development* **129**, 5789-5801.
- Giribet, G. (2003). Molecules, development and fossils in the study of metazoan evolution; Articulata versus Ecdysozoa revisited. *Zoology* **106**, 303-326.
- Giribet, G., Carranza, S., Baguna, J., Riutort, M. and Ribera, C. (1996). First molecular evidence for the existence of a Tardigrada + Arthropoda clade. *Mol. Biol. Evol.* **13**, 76-84.
- Giribet, G., Distel, D. L., Polz, M., Sterrer, W. and Wheeler, W. C. (2000). Triploblastic relationships with emphasis on the acoelomates and the position of Gnathostomulida, Cycliophora, Plathelminthes, and Chaetognatha: a combined approach of 18S rDNA sequences and morphology. *Syst. Biol.* **49**, 539-562.
- Hertzler, P. L. (2002). Development of the mesendoderm in the dendrobranchiate shrimp *Sicyoni ingentis*. *Arthropod Struct. Dev.* **31**, 33-49.
- Hertzler, P. L. and Clark, W. H., Jr (1992). Cleavage and gastrulation in the shrimp *Sicyonia ingentis*: invagination is accompanied by oriented cell division. *Development* **116**, 127-140.
- Hertzler, P. L., Wang, S. W. and Clark, W. H., Jr (1994). Mesendoderm cell and archenteron formation in isolated blastomeres from the shrimp *Sicyonia ingentis*. *Dev. Biol.* **164**, 333-344.
- Houthoofd, W., Jacobsen, K., Mertens, C., Vangestel, S., Coomans, A. and Borgonie, G. (2003). Embryonic cell lineage of the marine nematode *Pellioiditis marina*. *Dev. Biol.* **258**, 57-69.
- Hutter, H. and Schnabel, R. (1994). glp-1 and inductions establishing embryonic axes in *C. elegans*. *Development* **120**, 2051-2064.
- Inoue, I. (1958). Studies on the life history of *Chordodes japonensis*, a species of Gordiacea. I. The development and structure of the larva. *Jap. J. Zool.* **12**, 203-218.
- Kühn, A. (1913). Die Sondierung der Keimesbezirke in der Entwicklung der Sommereier von *Polyphemus*. *Zool. Jb. Anat.* **35**.
- Lang, K. (1953). Die Entwicklung des Eies von *Priapulius caudatus* Lam. und die systematische Stellung der Priapuliden. *Arkiv Zoologi* **5**, 321-348.
- Maas, A. and Waloszek, D. (2001). Cambrian derivatives of the early arthropod stem lineage, pentastomids, tardigrades and lobopodians – an 'Orsten' perspective. *Zool. Anz.* **240**, 451-459.
- Malakhov, V. V. and Spiridonov, S. E. (1984). The embryogenesis of *Gordius sp.* from Turkmenia, with special reference to the position of the Nematomorpha in the animal kingdom. *Zool. Zh.* **63**, 1285-1297.
- Mallatt, J. M., Garey, J. R. and Shultz, J. W. (2004). Ecdysozoan phylogeny and Bayesian inference: first use of nearly complete 28S and 18S rRNA gene sequences to classify the arthropods and their kin. *Mol. Phylogenet. Evol.* **31**, 178-191.
- Manton, S. M. (1949). Studies on the Onychophora VII. The early embryonic stages of Peripatopsis and some general considerations concerning the morphology and phylogeny of the Arthropoda. *Philos. Trans. R. Soc. B* **233**, 483-580.
- Marcus, E. (1928). Zur Embryologie der Tardigraden. *Verh. d. Deutsch. Zool. Ges.* **32**, 134-146.
- Marcus, E. (1929). Zur Embryologie der Tardigraden. *Zool. Jb. Anat.* **50**, 334-379.
- Meyer, N. T. (1913). Zur Entwicklung von *Gordius aquaticus*. *Z. wiss. Zool.* **105**, 125-136.
- Mühdorf, A. (1914). Beiträge zur Entwicklungsgeschichte und zu den phylogenetischen Beziehungen der Gordiuslarve. *Z. wiss. Zool.* **111**, 1-75.
- Nielsen, C. (2001). *Animal Evolution*. New York, NY: Oxford University Press.
- Nielsen, C. (2003). Proposing a solution of the Articulata-Ecdysozoa controversy. *Zoologica Scripta* **32**, 475-483.

- Regier, J. C. and Shultz, J. W.** (2001). Elongation factor-2: a useful gene for arthropod phylogenetics. *Mol. Phylogenet. Evol.* **20**, 136-148.
- Schneider, G.** (1976). Stadien der Embryonalentwicklung von *Eupagurus prideauxi* Leach (Crustacea, Decapoda, Anomura). *Zool. Jb. Anat.* **95**, 297-353.
- Schmidt-Rhaesa, A.** (2001). Tardigrades – Are they really miniaturized dwarfs? *Zool. Anz.* **240**, 549-555.
- Schmidt-Rhaesa, A., Bartolomaeus, T., Lemburg, C., Ehlers, U. and Garey, J. R.** (1998). The position of the arthropoda in the phylogenetic system. *J. Morph.* **238**, 263-285.
- Schnabel, R., Hutter, H., Moerman, D. and Schnabel, H.** (1997). Assessing normal embryogenesis in *Caenorhabditis elegans* using a 4D microscope: variability of development and regional specification. *Dev. Biol.* **184**, 234-265.
- Scholtz, G.** (1997). Cleavage, germ band formation and head segmentation: the ground pattern of the Euarthropoda. In *Arthropod Relationships* (ed. R. A. Fortey and R. H. Thomas), pp. 317-332. London, UK: Chapman & Hall.
- Scholtz, G.** (2002). The Articulata hypothesis – or what is a segment? *Org. Divers. Evol.* **2**, 197-215.
- Scholtz, G.** (2003). Is the taxon Articulata obsolete? Arguments in favour of a close relationship between annelids and arthropods. In *The New Panorama of Animal Evolution, Proceedings of the 18th International Congress of Zoology* (ed. A. Legakis, S. Sfenthourakis, R. Polymeni and M. Thessalou-Legaki), pp. 489-501. Sofia, Bulgaria: Pensoft.
- Scholtz, G.** (2004). Baupläne versus ground patterns, phyla versus monophyla: aspects of patterns and processes in evolutionary developmental biology. In *Evolutionary Developmental Biology of the Crustacea* (ed. G. Scholtz), pp. 3-16. Lisse, The Netherlands: A. A. Balkema.
- Siewing, R.** (1969). Lehrbuch der Vergleichenden Entwicklungsgeschichte der Tiere. Hamburg, Germany: Parey.
- Stollewerk, A.** (2002). Recruitment of cell groups through Delta/Notch signalling during spider neurogenesis. *Development* **129**, 5339-5348.
- Sulston, J. E. and Horvitz, H. R.** (1977). Post-embryonic cell lineages of the nematode, *Caenorhabditis elegans*. *Dev. Biol.* **56**, 110-156.
- Sulston, J. E., Schierenberg, E., White, J. G. and Thomson, J. N.** (1983). The embryonic cell lineage of the nematode *Caenorhabditis elegans*. *Dev. Biol.* **100**, 64-119.
- Tiegs, O. W.** (1940). The embryology and affinities of the Symphyla, based on a study of *Hanseniella agilis*. *Q. J. Microsc. Sci.* **82**, 1-225.
- Tiegs, O. W.** (1947). The development and affinities of the Pauropoda, based on a study of *Pauropus sylvaticus*. *Q. J. Microsc. Sci.* **88**, 165-267, 275-336.
- Urbach, R., Schnabel, R. and Technau, G. M.** (2003). The pattern of neuroblast formation, mitotic domains and proneural gene expression during early brain development in *Drosophila*. *Development* **130**, 3589-3606.
- Valentine, J. W.** (1997). Cleavage patterns and the topology of the metazoan tree of life. *Proc. Natl. Acad. Sci. USA* **94**, 8001-8005.
- von Erlanger, R.** (1895). Beiträge zur Morphologie der Tardigraden. I. Zur Embryologie eines Tardigraden: *Macrobotus macronyx* Dujardin. *Morph. Jb.* **22**, 491-513.
- von Wenck, W.** (1914). Entwicklungsgeschichtliche Untersuchungen an Tardigraden (*Macrobotus lacustris* Duj.). *Zool. Jb. Anat.* **37**, 465-514.
- Voronov, D. A.** (1999). The embryonic development of *Pontonema vulgare* (Enoplida: Onycholaimidea) with a discussion of nematode phylogeny. *Russ. J. Nematol.* **7**, 105-114.
- Voronov, D. A.** (2001). Comparative embryology of nematodes and the law of embryo similarity. *Zh. Obshch. Biol.* **62**, 34-48.
- Voronov, D. A. and Panchin, Y. V.** (1998). Cell lineage in marine nematode *Enoplus brevis*. *Development* **125**, 143-150.
- Weygoldt, P.** (1960). Embryologische Untersuchungen an Ostracoden: Die Entwicklung von *Cyprideis litoralis* (G. S. Brandy). Ostracoda, Podocopa; Cytheridae. *Zool. Jb. Anat.* **78**, 369-426.
- Weygoldt, P.** (1986). Arthropod interrelationships – the phylogenetic-systematic approach. *Z. Zool. Syst. Evolutionsforsch.* **24**, 19-35.
- Wiegner, O. and Schierenberg, E.** (1999). Regulative development in a nematode embryo: a hierarchy of cell fate transformations. *Dev. Biol.* **215**, 1-12.
- Wolff, C. and Scholtz, G.** (2002). Cell lineage, axis formation, and the origin of germ layers in the amphipod crustacean *Orchestia cavimana*. *Dev. Biol.* **250**, 44.
- Zhinkin, L.** (1949). Early stages in the development of *Priapulius caudatus*. *Dokl. Akad. Nauk SSSR* **65**, 409-412.
- Zhinkin, L. and Korsakova, G.** (1953). Early stages in the development of *Halicyptus spinulosus*. *Dokl. Akad. Nauk SSSR* **88**, 571-573.
- Zilch, R.** (1978). Embryologische Untersuchungen an der holoblastischen Ontogenese von *Penaeus trisulcatus* Leach (Crustacea, Decapoda). *Zoomorphologie* **90**, 67-100.
- Zilch, R.** (1979). Cell lineage in arthropods? *Fortschr. Zool. Syst. Evolutionsforsch.* **1**, 19-41.